

Facile synthesis and structure elucidation of metal-organic frameworks with {ZnCa} and {Zn₂Ca} metal cores

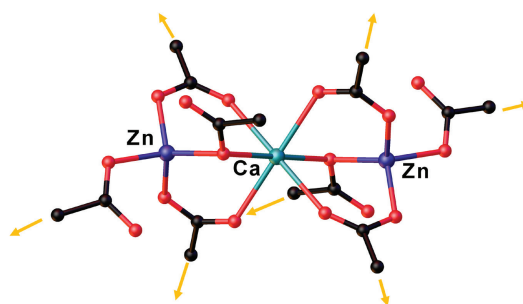
Irina K. Rubtsova,^a Stanislav N. Melnikov,^a Maxim A. Shmelev,^{*a} Stanislav A. Nikolaevskii,^{*a} Ilya A. Yakushev,^a Julia K. Voronina,^a Ekaterina D. Barabanova,^b Mikhail A. Kiskin,^a Alexey A. Sidorov^a and Igor L. Eremanko^a

^a N. S. Kurnakov Institute of General and Inorganic Chemistry, Russian Academy of Sciences, 119991 Moscow, Russian Federation. E-mail: shmelevma@yandex.ru, sanikol@igic.ras.ru

^b Samara Center for Theoretical Materials Science, Samara National Research University, 443011 Samara, Russian Federation

DOI: 10.1016/j.mencom.2020.11.011

The [ZnCa(DMF)₂(tda)₂]_n·nDMF and [Zn₂Ca(fda)₄]_n·2n(Me₂NH₂) metal-organic frameworks have been obtained by the reactions of pre-synthesized [Zn₂Ca(piv)₆(py)₂] (piv is pivalate, and py is pyridine) with 2,5-thiophenedicarboxylic (H₂tda) and 2,5-furandicarboxylic (H₂fda) acids, respectively. Complex [Zn₂Ca(piv)₆(py)₂] was used as a source of secondary building units with binuclear and trinuclear cores to form porous frameworks. The structure and topology of the compounds have been analyzed in detail.



Keywords: heterometallic coordination polymers, porous polymers, secondary building unit, X-ray structure, topology.

The on demand synthesis of metal-organic frameworks (MOFs) is fundamentally important because it is related to the opportunity of designing materials with tunable physico-chemical properties (permanent porosity, luminescent, magnetic and catalytic activity, etc.).^{1–9} Particularly, the development of synthetic procedures for heterometallic MOFs with controllable metal ion positions¹⁰ is of considerable current interest. This goal can be achieved by (i) the post-synthetic modification of MOFs, (ii) the simultaneous involving of different metal ions in MOF synthesis, and (iii) the coordination of heterometal ions by metalloligands. The advantages and drawbacks of these and some other approaches were analyzed in reviews.^{11,12} Two more advanced strategies using secondary building units (SBUs) in the rational synthesis of porous coordination polymers should be considered particularly. A stringent selection of SBUs and thoroughly verified co-doping technique of heterometal ions to the stable metal core allows targeted atomic arrangements within the SBU and makes it possible to achieve an electrocatalytic activity comparable to some multimetallic oxides.¹³ Another synthetic strategy deals with pre-synthesized discrete polynuclear complexes. This pathway is more predictable in comparison with a standard one-pot synthesis, and it provides opportunity to obtain MOFs inaccessible by self-assembly. The concept of heterometallic MOF production using discrete bimetallic pre-synthesized SBUs was recently developed.^{14–17} Here we present results of preliminary investigation of MOFs with {ZnCa} and {Zn₂Ca} metal cores. Despite this type of compounds possess luminescence properties^{18–21} and biological activity²² they are described in a limited number of publications. Previously, we found that the metal core of a heterometallic molecular complex can be fully preserved or partially rearranged upon treatment with a di- or tricarboxylic acid and an ancillary linker ligand depending on the particular

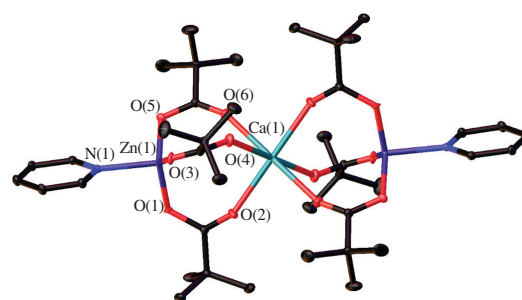
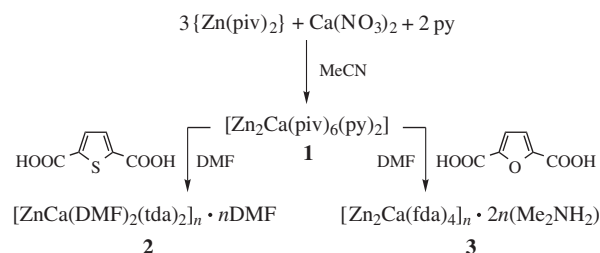


Figure 1 Molecular structure of complex 1. Hydrogen atoms are omitted for clarity.

carboxylate anion. The latter was exemplified by a number of 3d-Li and 3d-4f-heterometallic MOFs.^{14–17}

The first step to the synthesis of Zn–Ca polymers was to prepare the molecular complex [Zn₂Ca(piv)₆(py)₂] (**1**, Figure 1). Treatment of **1** with 2,5-thiophenedicarboxylic (H₂tda) or 2,5-furandicarboxylic (H₂fda) acids in DMF leads to the formation of neutral [ZnCa(DMF)₂(tda)₂]_n·nDMF (**2**, Figure 2) and ionic [Zn₂Ca(fda)₄]_n·2n(Me₂NH₂) (**3**, Figure 3) (Schemes 1 and S1) MOFs, respectively.



Scheme 1

Complex **2** is a framework based on a binuclear 7-connected $\{\text{ZnCa}(\text{DMF})_2(\text{OOC}-)_4\}$ heterometallic node [Figure 2(a)],[†] which was formed as a result of the partial destruction of complex **1**. Metal cations in a Zn–Ca fragment are connected by three bridging carboxylate anions. The Ca(1) ion completes its coordination environment to an octahedron (CaO_6) by the coordination of two DMF molecules. In a crystal of **2**, Zn–Ca fragments are linked in a chain by carboxylate bridges [Figure 2(b)]. In its turn, each chain is connected with five adjacent analogous chains by tda bridges. The porous framework formed 3,4,4,6T48 topological type in the standard representation of coordination networks (the centers of ligands and metals are nodes); its simplest topological motif of the topological type **pcu** was revealed from a cluster representation [Figure 2(c)]. The percentage of fully open channels was 17.3% (the volume was 496.1 Å³). The calculation was performed for potential guest molecule with 1.4 Å radii (Figure S1). The channels are isolated and filled by coordinated and solvated DMF molecules.

Similar networks were found in eight other coordination networks deposited in CSD (<https://topcryst.com>), for example, $[\text{CdCa}(\text{OH}-m\text{-BDC})_2(\text{H}_2\text{O})_2] \cdot 2\text{Me}_2\text{NH}$, where OH-*m*-H₂BDC is 5-hydroxyisophthalate.²⁷

The anionic framework $\{(\text{Zn}_2\text{Ca}(\text{fda})_4)^{2-}\}_n \cdot 2n(\text{Me}_2\text{NH}_2)$ **3** [Figure 3(a)] is based on the centrosymmetric 8-connected trinuclear linear fragment $\{\text{Zn}_2\text{Ca}(\text{fda})_2\}$. The central atom Ca(1) connected to terminal Zn(1) atoms by two μ_2 -bridging carboxylate groups and one $\mu_2\kappa^1$ -bridging O atom from an adjacent carboxylate

[†] Crystal data for **1**. $\text{C}_{40}\text{H}_{64}\text{CaN}_2\text{O}_{12}\text{Zn}_2$ ($M = 935.75$), $T = 150$ K, triclinic, space group $P\bar{1}$, $a = 10.3557(2)$, $b = 11.5542(3)$ and $c = 11.7790(2)$ Å, $\alpha = 63.0130(10)^\circ$, $\beta = 88.1410(10)^\circ$, $\gamma = 75.0250(10)^\circ$, $V = 1207.36(5)$ Å³, $Z = 1$, $\mu(\text{MoK}\alpha) = 1.155$ mm⁻¹. At the angles $2\theta < 29.00^\circ$, 13629 reflections were measured, including 6374 unique reflections ($R_{\text{int}} = 0.0297$) and 5185 reflections with $I > 2\sigma(I)$, which were used in the calculations. The final $R_1 = 0.0500$, $wR_2 = 0.0758$ (all data) and $R_1 = 0.0361$, $wR_2 = 0.0703$ [$I > 2\sigma(I)$], GOOF = 0.963. Largest diff. peak/hole 0.304 and -0.427 eÅ⁻³.

Crystal data for **2**. $\text{C}_{21}\text{H}_{25}\text{CaN}_3\text{O}_{11}\text{S}_2\text{Zn}$ ($M = 665.01$), $T = 100$ K, monoclinic, space group $P2_1/n$, $a = 8.7860(18)$, $b = 18.954(4)$ and $c = 17.604(4)$ Å, $\beta = 101.43(3)^\circ$, $V = 2873.5(10)$ Å³, $Z = 4$, $\mu(\text{MoK}\alpha) = 0.098$ mm⁻¹. At the angles $1.78^\circ < 2\theta < 30.96^\circ$, 34603 reflections were measured, including 6496 unique reflections ($R_{\text{int}} = 0.0557$) and 5568 reflections with $I > 2\sigma(I)$, which were used in the calculations. The final $R_1 = 0.0472$, $wR_2 = 0.1126$ (all data) and $R_1 = 0.0401$, $wR_2 = 0.1077$ [$I > 2\sigma(I)$], GOOF = 1.080. Largest diff. peak/hole 1.101 and -0.532 eÅ⁻³.

Crystal data for **3**. $\text{C}_{28}\text{H}_{24}\text{CaN}_2\text{O}_{20}\text{Zn}_2$ ($M = 879.31$), $T = 100$ K, monoclinic, space group $P2_1/c$, $a = 9.4230(19)$, $b = 15.748(3)$ and $c = 17.354(4)$ Å, $\beta = 90.77(3)^\circ$, $V = 2575.0(9)$ Å³, $Z = 2$, $\mu(\text{MoK}\alpha) = 0.098$ mm⁻¹. At the angles $1.95^\circ < 2\theta < 28.92^\circ$, 16991 reflections were measured, including 4830 unique reflections ($R_{\text{int}} = 0.0476$) and 3733 reflections with $I > 2\sigma(I)$, which were used in the calculations. The final $R_1 = 0.0782$, $wR_2 = 0.1806$ (all data) and $R_1 = 0.0654$, $wR_2 = 0.1735$ [$I > 2\sigma(I)$], GOOF = 1.283. Largest diff. peak/hole 0.711 and -1.530 eÅ⁻³.

The XRD analysis of **1** was accomplished on a Bruker APEX-II diffractometer using a standard procedure (MoK α -irradiation, graphite monochromator, $\lambda = 0.71073$ Å, ω -scans with 1° step). X-ray diffraction data for **2** and **3** were collected on the ‘Belok’ beamline of the Kurchatov Synchrotron Radiation Source (National Research Center ‘Kurchatov Institute’, Moscow, Russian Federation) in φ -scan mode with 1° step ($\lambda = 0.79312$ Å) using Rayonix SX165 CCD detector at 100 K.²³ The data were indexed, integrated and scaled using the XDS program suite.²⁴ Using Olex2,²⁵ the structures were solved with the ShelXS structure solution program using direct methods and refined using the ShelXL²⁶ refinement package with the least squares minimization in an anisotropic approximation for nonhydrogen atoms. The H atoms were added in the calculated positions and refined using the riding model in an isotropic approximation.

CCDC 2010502–2010504 contain supplementary crystallographic data for this paper. These data can be obtained free of charge from The Cambridge Crystallographic Data Centre via <http://www.ccdc.cam.ac.uk>.

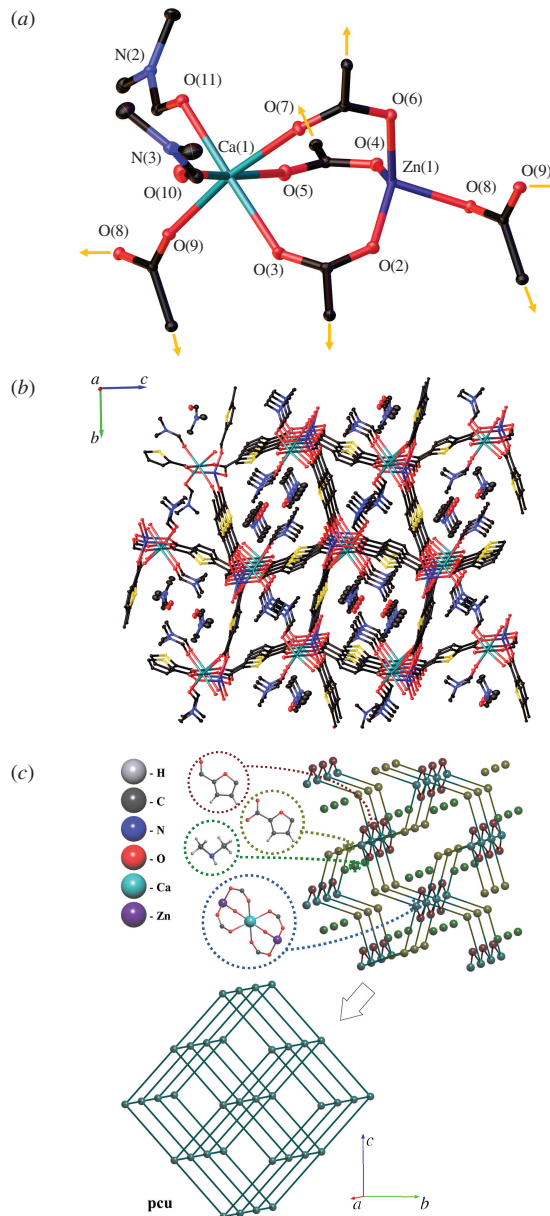


Figure 2 (a) Binuclear 7-connected fragment, (b) a fragment of molecular packing in the crystal, and (c) simplification of the structure to underlying net in the cluster representation with **pcu** topology for **2**.

group. Each trinuclear framework is connected with eight adjacent analogous fragments by fda linkers. The underlying net formed [Figure 3(b)] belongs to the topological type 4,4,4T27 [in standard representation, Figure 3(c)], which has been found in 14 other coordination polymers with linear naphthalene-1,4-dicarboxylate and benzene-1,4-dicarboxylate linkers. Thus, tda with larger angle (151.81 and 152.66°) in comparison to fda (134.36 and 131.81–135.80°) leads to a framework similar to linear linkers. Cluster representation of the compound leads to the underlying net with a topology of 3,5-c **gra** by simplification of dimeric SBU and thiophene carboxylate into 5-c and 3-c nodes, respectively. The charge of anionic framework is compensated by Me_2NH_2^+ cations, which formed upon DMF decomposition. This is a typical case of DMF acid hydrolysis under solvothermal conditions.^{20,28,29} In the packing of **3**, a network of cavities is formed, which consists of two penetrating one-dimensional connected channels parallel to the axes *a* and *c* (Figure S2). The percentage of fully open channels was 43.9% (calculated for potential guest molecule with 1.4 Å radii). The channels were filled with Me_2NH_2^+ cations and DMF molecules which were squeezed from final refinement because of disordering.

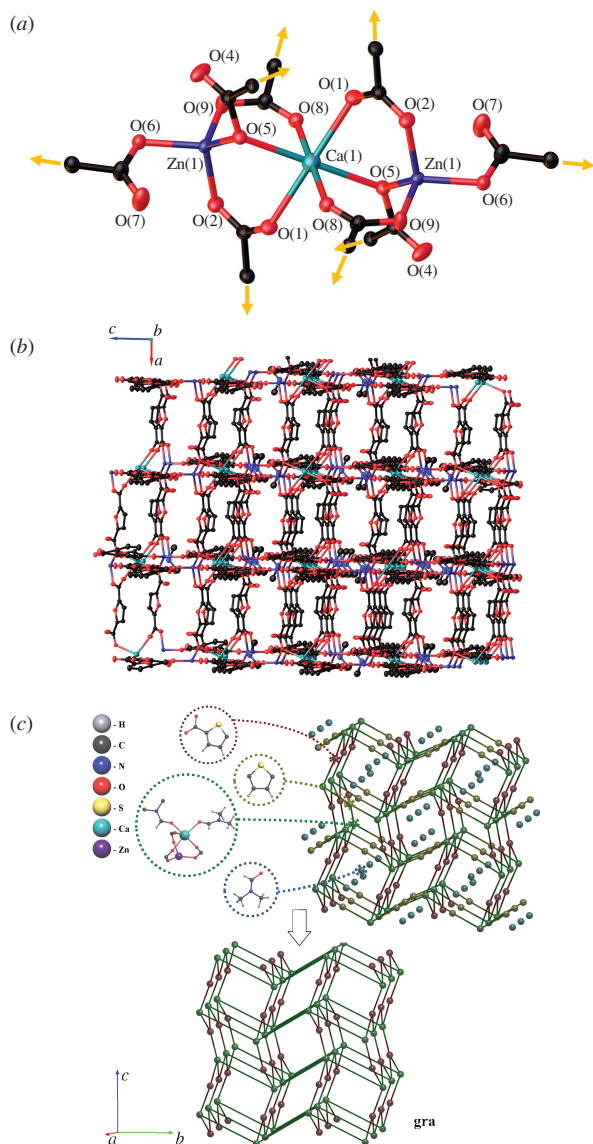


Figure 3 (a) Trinuclear 8-connected fragment $\{Zn_2Ca(OOC^-)_8\}$, (b) the fragment of molecular packing in the crystal, and (c) the structure simplification in the cluster representation to 3,5-c net of *gra* topology for **3**.

The anionic fda-based frameworks isostructural to compound **3** were described earlier for homometallic zinc complexes.^{30,31} A similar anionic framework $[Cd_2Ca(Bu^l-m-BDC)_4] \cdot 2(Me_2NH_2)$ based on a 8-connected trinuclear fragment with anions of 5-*tert*-butylisophthalic acid (Bu^l-m-H_2BDC) was reported previously.²⁷ All these MOFs were synthesized solvothermally from inorganic zinc and calcium salts while pre-synthesized SBUs have never been used for the production of heterometallic Zn–Ca MOFs.

Thus, this work provides a rational synthetic strategy for the construction of novel heterometallic functional materials with dicarboxylate ligands.

This work was supported by the Russian Foundation for Basic Research (grant no. 18-29-04043). The X-ray structural studies (compound **1**), elemental analysis and IR spectroscopy were performed using shared experimental facilities supported by IGIC RAS state assignment. EDB acknowledges the Russian Science Foundation (grant no. 18-73-10116) for financial support of the development of the methods of topological analysis.

Online Supplementary Materials

Supplementary data associated with this article can be found in the online version at doi: 10.1016/j.mencom.2020.11.011.

References

- 1 Y.-S. Wei, L. Sun, M. Wang, J. Hong, L. Zou, H. Liu, Y. Wang, M. Zhang, Z. Liu, Y. Li, S. Horike, K. Suenaga and Q. Xu, *Angew. Chem., Int. Ed.*, 2020, **59**, 16013.
- 2 M. Mon, R. Bruno, S. Sanz-Navarro, C. Negro, J. Ferrando-Soria, L. Bartella, L. Di Donna, M. Prejanò, T. Marino, A. Leyva-Pérez, D. Armentano and E. Pardo, *Nature Commun.*, 2020, **11**, 3080.
- 3 D. Aulakh, L. Liu, J. R. Varghese, H. Xie, T. Islamoglu, K. Duell, C.-W. Kung, C.-E. Hsiung, Y. Zhang, R. J. Drout, O. K. Farha, K. R. Dunbar, Y. Han and M. Wriedt, *J. Am. Chem. Soc.*, 2019, **141**, 2997.
- 4 A. A. Lysova, D. G. Samsonenko, P. V. Dorovatovskii, V. A. Lazarenko, V. N. Khrustalev, K. A. Kovalenko, D. N. Dybtsev and V. P. Fedin, *J. Am. Chem. Soc.*, 2019, **141**, 17260.
- 5 D. N. Dybtsev, A. A. Sopianik and V. P. Fedin, *Mendeleev Commun.*, 2017, **27**, 321.
- 6 L. M. Kustov, V. I. Isaeva, J. Přeck and K. K. Bisht, *Mendeleev Commun.*, 2019, **29**, 361.
- 7 L. M. Tijerina, C. M. O. González, B. I. Kharisov, T. E. S. Quezada, Y. P. Méndez, O. V. Kharissova and I. G. de la Fuente, *Mendeleev Commun.*, 2019, **29**, 400.
- 8 J. Cui, M. Zhang, C. Wei, J. Zhu, X. Wang and X. Du, *Mendeleev Commun.*, 2020, **30**, 282.
- 9 A. A. Simagina, M. V. Polynski, A. V. Vinogradov and E. A. Pidko, *Russ. Chem. Rev.*, 2018, **87**, 831.
- 10 C. Castillo-Blas, V. A. de la Peña-O'Shea, I. Puente-Orench, J. R. de Paz, R. Sáez-Puche, E. Gutiérrez-Puebla, F. Gándara and Á. Monge, *Sci. Adv.*, 2017, **3**, e1700773.
- 11 M. Y. Masoomi, A. Morsali, A. Dhakshinamoorthy and H. Garcia, *Angew. Chem., Int. Ed.*, 2019, **58**, 15188.
- 12 A. A. Sopianik and V. P. Fedin, *Russ. J. Coord. Chem.*, 2020, **46**, 443 (*Koord. Khim.*, 2020, **46**, 387).
- 13 C. Castillo-Blas, N. López-Salas, M. C. Gutiérrez, I. Puente-Orench, E. Gutiérrez-Puebla, M. L. Ferrer, M. Á. Monge and F. Gándara, *J. Am. Chem. Soc.*, 2019, **141**, 1766.
- 14 A. A. Sopianik, I. A. Lutsenko, M. A. Kiskin, A. A. Sidorov, I. L. Eremenko, D. G. Samsonenko, D. N. Dybtsev and V. P. Fedin, *Russ. Chem. Bull., Int. Ed.*, 2016, **65**, 2601 (*Izv. Akad. Nauk, Ser. Khim.*, 2016, 2601).
- 15 A. A. Sopianik, E. N. Zorina-Tikhonova, M. A. Kiskin, D. G. Samsonenko, K. A. Kovalenko, A. A. Sidorov, I. L. Eremenko, D. N. Dybtsev, A. J. Blake, S. P. Argent, M. Schröder and V. P. Fedin, *Inorg. Chem.*, 2017, **56**, 1599.
- 16 A. A. Sopianik, M. A. Kiskin, D. G. Samsonenko, A. A. Ryadun, D. N. Dybtsev and V. P. Fedin, *Polyhedron*, 2018, **145**, 147.
- 17 A. A. Sopianik, M. A. Kiskin, K. A. Kovalenko, D. G. Samsonenko, D. N. Dybtsev, N. Audebrand, Y. Sun and V. P. Fedin, *Dalton Trans.*, 2019, **48**, 3676.
- 18 J.-C. Zhang, J.-J. Wang, S.-L. Zeng, Z.-M. Wang, Y. Liu, D.-J. Zhang, R.-C. Zhang and Y. Fan, *Inorg. Chem. Commun.*, 2018, **97**, 69.
- 19 X. Zhang, Y.-Y. Huang, J.-K. Cheng, Y.-G. Yao, J. Zhang and F. Wang, *CrystEngComm*, 2012, **14**, 4843.
- 20 D.-L. Yang, X. Zhang, J.-X. Yang, Y.-G. Yao and J. Zhang, *Inorg. Chim. Acta*, 2014, **423**, 62.
- 21 A. Ablet, S.-M. Li, W. Cao, X.-J. Zheng and L.-P. Jin, *Polyhedron*, 2014, **83**, 122.
- 22 A. A. Alie El-Deen, A. El-Monem, E. El-Askalany, R. Halaoui, B. J. Jean-Claude, I. S. Butler and S. I. Mostafa, *J. Mol. Struct.*, 2013, **1036**, 161.
- 23 R. D. Svetogorov, P. V. Dorovatovskii and V. A. Lazarenko, *Cryst. Res. Technol.*, 2020, **55**, 1900184.
- 24 W. Kabsch, *Acta Crystallogr.*, 2010, **D66**, 125.
- 25 O. V. Dolomanov, L. J. Bourhis, R. J. Gildea, J. A. K. Howard and H. Puschmann, *J. Appl. Crystallogr.*, 2009, **42**, 339.
- 26 G. M. Sheldrick, *Acta Crystallogr.*, 2015, **C71**, 3.
- 27 J.-D. Lin, S.-T. Wu, Z.-H. Li and S.-W. Du, *Dalton Trans.*, 2010, **39**, 10719.
- 28 Z. Zhang and M. J. Zaworotko, *Chem. Soc. Rev.*, 2014, **43**, 5444.
- 29 R. Medishetty, V. Nalla, L. Nemeč, S. Henke, D. Mayer, H. Sun, K. Reuter and R. A. Fischer, *Adv. Mater.*, 2017, **29**, 1605637.
- 30 S. S. Nagarkar, A. K. Chaudhari and S. K. Ghosh, *Cryst. Growth Des.*, 2012, **12**, 572.
- 31 H.-H. Li, W. Shi, N. Xu, Z.-J. Zhang, Z. Niu, T. Han and P. Cheng, *Cryst. Growth Des.*, 2012, **12**, 2602.

Received: 27th July 2020; Com. 20/6272